Fuel 362 (2024) 130747

Contents lists available at ScienceDirect

Fuel

journal homepage: www.elsevier.com/locate/fuel

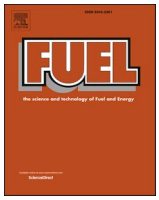

Full Length Article

Detailed kinetic analysis of synthetic fuels containing ammonia

Gianmaria Pio [a,*], Sven Eckart [b], Andreas Richter [c], Hartmut Krause [b], Ernesto Salzano [a]

[a] Department of Civil, Chemical, Environmental and Materials Engineering, Alma Mater Studiorum - University of Bologna, Bologna 40131, Italy
[b] Institute of Thermal Engineering, TU Bergakademie Freiberg, Freiberg 09599, Germany
[c] Institute of Energy Process Engineering and Chemical Engineering, TU Bergakademie Freiberg, Freiberg 09599, Germany

ARTICLE INFO

Keywords:
Synthetic fuels
Kinetic mechanisms
Laminar burning velocity
Flammability limits
Additivity correlations

ABSTRACT

The imperative to adopt environmentally sustainable energy sources has propelled the exploration of zero-carbon alternatives, such as hydrogen and ammonia for energy supply. Integrating these species with methane is recognized as a viable short-term solution. However, a complete understanding of their chemical behaviour in a wide range of conditions remains elusive, especially in terms of safety parameters, limiting the applicability of this solution. To this aim, this work presents a detailed analysis of the overall reactivity, expressed either in terms of laminar burning velocity or flammability limits, of hydrogen-ammonia-containing fuels. Additional considerations were obtained by the analysis of the maximum pressure rise and maximum pressure obtained in adiabatic conditions. A spectrum of nitrogen/oxygen mixtures was scrutinized, and the influence of initial temperature within the range of 300–500 K was systematically investigated. The estimation quality of the adopted mechanism was evaluated by comparing numerical predictions with experimental measurements obtained by different systems, when available. A tendency in slightly more conservative results on the safe side was detected for the assessment of flammability limits and minimum oxygen concentration. This trend was attributed to the assumption of perfectly adiabatic conditions posed for the numerical analysis, which does not perfectly match the experimental conditions. Conversely, an excellent agreement between numerical and experimental laminar burning velocity was observed. Therefore, the collected data were used for the quantification of input parameters required by well-established correlations suitable for synthetic fuels.

1. Introduction

In the framework of energy transition and innovation in critical phases of the energy supply chain, the last decades have been characterized by increased attention on environmental aspects towards cleaner fuels and technological solutions [1]. The abovementioned trend has been additionally promoted by global economic and socio-political factors. Indeed, the well-known fluctuations in traditional fuel prices have pushed toward the utilization of alternative solutions in several industrial fields. A clear example of this tendency is the integration of clean and clean-up technologies in industrial processes devoted to the production of innovative energy sources, leading to the introduction of a large set of alternative substances or mixtures [2]. Among the others, hydrogen-containing mixtures and ammonia-containing mixtures are worth specific mention. The blending of hydrogen and ammonia with methane/natural gas is considered a short- and medium-term solution for the energy sector [3]. In addition, methane can be also considered as the main component of synthetic natural gas, making mixtures based on ammonia-methane-hydrogen a potential synthetic fuel.

Once focusing on the energy production phase, considering the chemical properties of each species composing these mixtures, an increase in ammonia may lead to insufficient overall reactivity [4], conversely, the addition of hydrogen in methane has a limited impact until elevated content of hydrogen is reached [5,6]. In this sense, the use of oxygen-enriched air can compensate for the abovementioned drop in overall reactivity caused by the addition of ammonia [7]. Hence, the oxygen-to-nitrogen ratio within the oxidant mixture can be intended as an additional operative condition to be optimized together with the initial composition of the adopted fuel mixture. From this perspective, it is worth mentioning that several alternatives for air separation processes exist [8]. Although the techno-economic feasibility of air separation plants is strongly affected by the size of the plant, oxygen-enriched air having an oxygen content of up to 40 %v can be conveniently produced as a by-product of high-pure nitrogen processes based on the use of membranes, suggesting its utilization on an industrial scale for energy production [8].

* Corresponding author.
E-mail address: gianmaria.pio@unibo.it (G. Pio).

https://doi.org/10.1016/j.fuel.2023.130747
Received 30 October 2023; Received in revised form 11 December 2023; Accepted 23 December 2023
Available online 5 January 2024

The unique chemical structure and potential initial composition variations necessitate dedicated studies to assess the adequacy of current models and infrastructure either in terms of normal operations or safety considerations. However, to the best of our knowledge, either experimental or numerical investigations on the kinetic aspects and safety parameters of hydrogen-ammonia-methane mixtures are missing. In this view, modelling physical and chemical aspects of gaseous mixtures from a fundamental-oriented perspective is essential to fully reproduce the occurring phenomena in a wide range of conditions. Indeed, previous studies have reported that the commonly adopted correlations and estimation strategies bring elevated levels of uncertainties and inaccuracy when hydrogen is introduced in a gaseous mixture [9,10], because of the possible interactions between decomposition pathways and small radicals [11]. For these reasons, the use of detailed kinetic mechanisms has been largely promoted for the investigation of the additivity effects on the overall reactivity of light species. Kinetic mechanisms consist of a list of thermodynamic and kinetic parameters governing radical-level elemental steps. Data collection methods encompass experimental, theoretical (e.g., quantum mechanical calculations), or empirical approaches. Typically, the need for the quantification of short-living species, such as radicals, imposes the use of demanding experimental techniques [12]. In the absence of experimental data, theoretical calculations are favoured, albeit being a time-intensive undertaking [13]. Additional information on the theoretical background related to this numerical approach can be found in the dedicated literature [14]. Correlations, like Benson's group additivity method, inferential methods, or machine learning, can provide the missing data based on chemical structure similarities [15,16]. Once the databases are considered, kinetic mechanisms can be distinguished in terms of strategies, such as manual updates or automated generation algorithms [17,18], adopted for their realization of in terms sizes, being classified as detailed, reduced, or skeletal. Taking into account the numerical nature of the kinetic mechanisms, sound validation of kinetic mechanisms is essential against extended and reliable experimental sets of data. To this aim, particular emphasis on the laminar burning velocity has been given as a pivotal parameter [19], as it encompasses crucial information pertaining to reactivity, thermal properties, flame morphology, and geometric characteristics [20–22]. Several experimental systems can be adopted for the quantification of the laminar burning velocity, including the Bunsen burner [23], counter-flow flame [24], spherical bomb [25], annular stepwise diverging tube [26,27], and heat flux burner [28,29], as described in detail elsewhere [30–33].

Once focusing on the safety aspects of these fuels, it is worth noting that the low density of these substances imposes a high level of compression or the implementation of cryogenic conditions for a convenient transportation system [34], resulting in a substantial surge of interest in the characterization of the low-temperature behaviour of light compounds [35]. The acquired knowledge in the field of chemical kinetics can be adopted for the evaluation of safety aspects involving synthetic fuels under consideration in this work. To this aim, the limiting laminar burning velocity theory [36] and the calculated adiabatic flame temperature theory [37] are eminent examples of possible strategies for the numerical estimation of flammability limits [38]. Considering the current status of the available technologies, a compressed gas solution can be assumed as a possible storage and transportation system for the investigated mixtures [39]. Therefore, in the case of a continuous accidental release, a chocked flow potentially results in jet fires or flash fires, contingent upon the presence of an ignition source [40]. In both scenarios, the proximity of the release is characterized by heightened turbulence and sudden variations in flow properties, making the description and modelling of the main phenomena challenging. To cope with this, an under-expanded jet can be represented by a Mach disk, aiding in the assessment of the boundary conditions to be considered for the consequence analysis [41]. In this sense, a single value for initial pressure can be considered for the evaluation of the most relevant parameters necessary to quantify the consequences of these scenarios. In addition, the evaluation of safety parameters is essential for the characterization of possible scenarios resulting from delayed ignition as well as the definition of optimized operative conditions in industrial processes [42]. It is well established that flammability limits exhibit significant variation, primarily with initial temperature. Bearing in mind the storage conditions and physical properties of the substances under investigation, a low initial temperature can be expected [43]. However, the presence of possible hot surfaces can be often considered as a possible source of ignition, leading – even locally – to increases in temperatures. The specific temperature of hot surfaces is significantly affected by the investigated facility. Nevertheless, a maximum initial temperature of 500 K for gaseous mixtures can be considered to be representative of the low-temperature range on the safe side [44].

For these reasons, this work was focused on the characterization of the effects of initial composition on the laminar burning velocity and flammability limits of hydrogen-ammonia-methane mixtures in air. Further insights were acquired on safety aspects relevant for the evaluation of consequences due to the accidental release of these gaseous mixtures whether an ignition source is present or not as well as in a closed or open atmosphere. Based on the collected data, a simplified correlation assessing the overall reactivity as a function of initial fuel composition, initial oxidant composition, fuel-to-oxygen ratios and initial temperature will be produced and trained. The obtained findings can be, thus, intended also as a paramount step toward the implementation of kinetic models within advanced numerical tools (e.g., computational fluid dynamics) as well as for an accurate quantitative risk assessment of systems based on gaseous synthetic fuels and their blends.

2. Methodology

In this work, a detailed kinetic mechanism (Kinetic in Bologna, KIBO) validated for light species, including either light hydrocarbons or nitrogen-based chemistry [45] was used. The adopted kinetic mechanism includes 172 species and 488 reactions. The design of KIBO prioritizes final size and computational efficiency for practical implementation while maintaining accuracy, as evidenced by thorough validation documented in existing literature [5]. A zero-dimensional reactor implemented in the open-source software Cantera [46], was utilized to represent the adiabatic conditions in a transient mode. The grid refining criteria were chosen as ratio = 3, slope = 0.05, curve = 0.07 after a comprehensive grid sensitivity analysis, striking a balance between computational demands and accuracy. Previously performed grid sensitivity analyses have suggested a maximum slope and curve of 0.07 for extremely low temperatures [35]. However, preliminary investigations performed in this work demonstrated that a negligible impact on the obtained values and computational requirements can be observed once the slope is tightened to 0.05, suggesting its implementation to guarantee enhanced robustness data. Different initial temperatures, representative of low-temperature conditions, were investigated. More specifically, initial temperatures included within the range of 300 K – 500 K were studied. Conversely, an initial pressure of 1 bar was considered, exclusively. Concerning the composition, CH_4, NH_3, and H_2 were considered as fuel species in this work. Binary and ternary fuel mixtures containing hydrogen, ammonia, and methane as reported in Fig. 1, were analysed. Several initial compositions of fuel mixture were selected for this analysis to be representative of possible ratios between constituting fuels related to plausible strategies in their blending *in situ* as well as different readiness levels of the existing infrastructures [47]. More specifically, fuel mixtures having a Wobbe index (WI) within 21 – 46.5 were considered. WI was calculated following the definitions provided by the international standard ISO 6976:2016 [48] and assuming normal conditions.

In this sense, it is worth noting that the WI does not include any effects of the oxidant composition, by definition. This means that the possible use of oxygen-enriched air can partially compensate for a lower

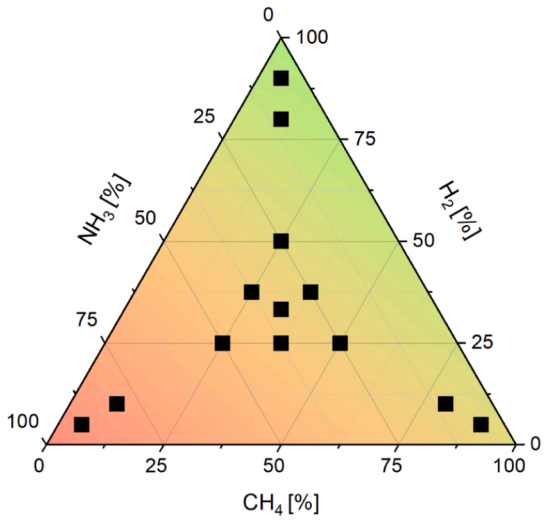

Mixture	CH_4 [%v]	H_2 [%v]	NH_3 [%v]	WI [MJ/Nm^3]
Mix 1	100	0	0	48.19
Mix 2	0	100	0	40.74
Mix 3	0	0	100	19.99
Mix 4	50	50	0	41.75
Mix 5	0	50	50	22.75
Mix 6	50	0	50	32.50
Mix 7	33.33	33.33	33.34	46.07
Mix 8	90	5	5	35.37
Mix 9	5	90	5	21.55
Mix 10	5	5	90	43.88
Mix 11	80	10	10	33.30
Mix 12	10	80	10	23.19
Mix 13	10	10	80	32.12
Mix 14	50	25	25	28.81
Mix 15	25	50	25	32.79
Mix 16	25	25	50	30.22
Mix 17	37.5	25	37.5	34.54
Mix 18	25	37.5	37.5	48.19
Mix 19	37.5	37.5	25	40.74

Fig. 1. Initial composition of the fuels investigated in this work.

WI because of the reduction in inert species (i.e., nitrogen) within the initial fuel-oxidant mixture. Therefore, the estimation of the laminar burning velocity (S_L) was performed as a function of the equivalence ratio (φ), defined in Eq. (1), and the air enrichment index (E), as reported in Eq. (2). Besides, additional safety parameters, such as the maximum pressure P_{max} and the maximum pressure rise rate $\left(\frac{dP}{dt}\right)_{max}$, were calculated to account for the case of accidental release in a closed or confined space.

$$\varphi = \sum_i \frac{\left(\frac{m_{Fi}}{m_{O_2}}\right)}{\left(\frac{\nu_{F_i}}{\nu_{O_2}}\right)} = \frac{\left(\frac{m_{CH_4}}{m_{O_2}}\right)}{\left(\frac{\nu_{CH_4}}{\nu_{O_2}}\right)} + \frac{\left(\frac{m_{H2}}{m_{O_2}}\right)}{\left(\frac{\nu_{H_2}}{\nu_{O_2}}\right)} + \frac{\left(\frac{m_{NH3}}{m_{O_2}}\right)}{\left(\frac{\nu_{NH_3}}{\nu_{O_2}}\right)} \quad (1)$$

$$E = \frac{m_{O_2}}{m_{N_2} + m_{O_2}} \quad (2)$$

where m_{Fi}, m_{CH_4}, m_{H_2}, m_{NH_3} m_{O_2}, and m_{N2} represent the molar fraction of the i-th fuel species, methane, hydrogen, ammonia, oxygen, and nitrogen in the unburned mixture, respectively. Similarly, ν_{F_i} ν_{CH_4}, ν_{H_2}, ν_{NH_3} and ν_{o_2} are intended as the stoichiometric coefficients of the i-th fuel, methane, hydrogen, ammonia, and oxygen in the reactions of complete oxidation. The maximum E investigated in this work was equal to 0.40, in compliance with the techno-economic analysis of the air separation processes reported in the literature [49].

Furthermore, the estimated S_L was considered for the evaluation of the flammability limits, following the limiting laminar burning velocity ($S_{L,lim}$) theory proposed by Hertzberg [36]. To this aim, the critical adiabatic flame temperature (CAFT) approach was adopted as per comparison [50]. More specifically, the lower (LFL) and upper flammability limits (UFL) were assumed as the compositions resulting in a laminar burning velocity equal to the $S_{L,lim}$ or in case the adiabatic flame temperature equals a critical value depending on the initial temperature. Namely, the threshold for the CAFT was assumed to be equal to the initial temperature + 900 K, as indicated in the literature for rough estimations [51]. For the sake of completeness, the adiabatic flame temperatures obtained once S_L is equal to $S_{L,lim}$ were evaluated, as well. Similarly, the threshold value of $S_{L,lim}$ is itself a function of initial composition and conditions, as defined in Eq. (3).

$$S_{L,lim} = \sqrt[3]{2\alpha g \frac{\rho_b}{\rho_u}} \quad (3)$$

where ρ_u and ρ_b are the unburned and burned gas density, respectively, whereas α is the thermal diffusivity of the gaseous mixture and g is the gravitational acceleration. Air was assumed as the oxidant agent, at first. Then, the oxygen-to-nitrogen ratio was modified for the estimation of the limiting oxygen concentration (LOC) and flammability limits for oxygen-enriched air. The estimation of the required thermodynamic and transport properties of the unburned and burned mixtures was performed through the same detailed kinetic mechanism adopted for the evaluation of the S_L.

3. Results and discussion

In this work, adiabatic flame temperature, laminar burning velocity and flammability limits were estimated as a function of initial fuel composition, fuel-to-oxidant ratio, oxygen content, and temperature. For the sake of conciseness, the full set of collected data is reported in supplementary material, whereas a part of them was included in the manuscript to elucidate the effects of boundary conditions on the investigated properties. More specifically, Figures S1 – S19 report the estimated adiabatic flame temperature as a function of the equivalence ratio for the investigated fuel mixtures at different initial temperatures and for the whole set of equivalence ratios. Conversely, Figures S20 – S38 show the effects of the equivalence ratio at extreme compositions (i.e., close to flammability limits), the initial composition of fuel and oxidant, and the initial temperature on the laminar burning velocity; eventually, the flammable region of the investigated mixtures are reported in Figure S39 for the analysed conditions.

3.1. Oxidation of pure fuels

In this subsection results related to pure fuel (i.e., Mix 1, Mix 2, and Mix 3) in oxygen/nitrogen will be discussed. The adopted kinetic mechanism has been intensively validated among experimental data collected at temperature and pressure relevant for the current investigation only for mixtures containing methane and hydrogen [5]. Therefore, a preliminary step devoted to the comparison of numerical and experimental data is presented in this work exclusively for the case of pure ammonia. To this aim, the collected data for the laminar burning velocity of ammonia in air at 300 K is presented (Fig. 2), at first. The experimental data considered for this analysis were reported by Pfahl et al. [52] and Takizawa et al. [53], as collected employing closed vessel microgravity (CVM), closed vessel (CV), and spherical vessel (SV) methods.

The reported data highlight the tendency to slightly overestimate the laminar burning velocity of ammonia-air mixtures. However, it is noteworthy that the observed oscillations are notably subdued in

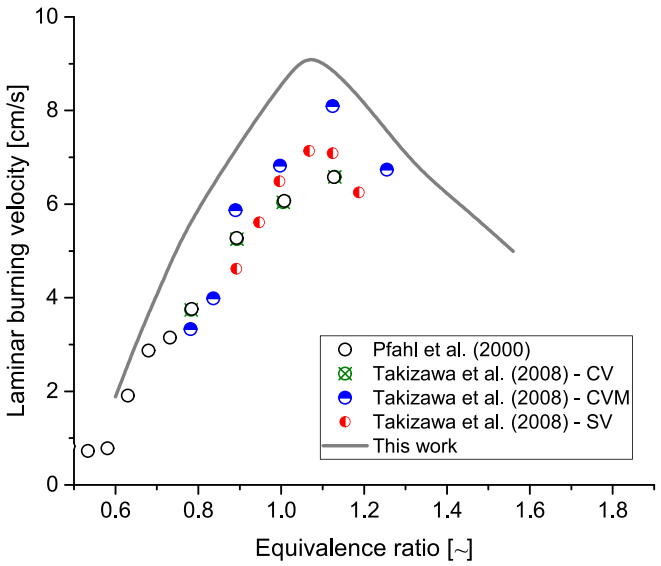

Fig. 2. Comparison of experimental and numerical laminar burning velocity for ammonia-air mixtures at an initial temperature of 300 K and initial pressure of 1 bar, as a function of the equivalence ratio.

comparison to those documented in a comprehensive recent literature review [54] about the laminar burning velocity of mixtures rich in ammonia encompassing various models. Considering the relative deviation between numerical and experimental data, the discrepancies between numerical and experimental datasets are more relevant in lean compositions. On the other hand, a significant variability can be observed among measurements reported for rich compositions deriving from different setups, possibly due to systematic errors, thus limiting the robustness of the accuracy of the adopted mechanism. Indeed, different approaches and correction parameters can be adopted for data refining dealing with laminar flames, leading to significant uncertainties associated with laminar burning velocity [30]. Similar considerations have been drawn by the comparison of the estimations obtained for pure methane and hydrogen (i.e., Mix 1 and Mix 2) in the air with experimental data available in the current literature [10]. However, it should be noted that the belt-shape profile as well as the conditions resulting in a peak in the laminar burning velocity are fairly reproduced by the kinetic mechanism. Therefore, the comparison of numerical and experimental data was extended to the flammability limits of ammonia in the presence of nitrogen–oxygen mixtures, as reported in Fig. 3. The experimental data collected by Kondo et al. [55] were included in this scope.

According to the reported data, KIBO tends to overestimate the lower flammability limits (LFLs). This trend is in line with the observations reported for the laminar burning velocity, where the estimated reactivity was larger than the measured one for lean mixtures. Conversely, the upper flammability limits (UFLs) are almost perfectly reproduced by the numerical approach, demonstrating the suitability of the selected mechanism for the description of ammonia chemistry. Indeed, it should be considered that a higher relevance of chemical kinetic is attributed to UFL than LFL, whereas thermal properties and boundary conditions typically determine the LFL [56]. This aspect can be considered if the refining of the kinetic mechanism is of concern as well as for the definition of a more robust set of boundary conditions. In this light, improved exchange coefficients as well as the refinement of the thermal boundary conditions can support a better reproduction of LFL, as well. Among the others, adiabatic conditions were assumed for the numerical case, whereas the experimental system can have non-negligible heat exchange with the surrounding environment, leading to less conservative results. Under this impulse, the kinetic mechanism was adopted for the evaluation of the selected mixtures containing hydrogen, methane, and/or ammonia, as discussed in the following sections.

3.2. Oxidation of binary mixtures

Following the definition of the initial mixtures previously provided in Fig. 1, estimations obtained for Mix 4, Mix 5, and Mix 6 will be reported and discussed within this subsection. Fig. 4 illustrates the evolution of the addition of CH_4 and H_2 to NH_3, focusing exclusively on the stoichiometric ratio under atmospheric conditions. For the sake of conciseness, a wider set of data including laminar burning velocities calculated at different equivalence ratios is reported in the supplementary material, exclusively.

It is evident that the introduction of hydrogen in ammonia results in a nonlinear, steadily increasing trend. From a quantitative perspective, two different areas can be identified. Indeed, the impact of hydrogen content assumes an exponential trend starting from 60 % of hydrogen. Conversely, the collected data indicate that methane addition to ammonia leads to a more linear trend in laminar burning velocity. However, it is worth noting that literature data from the years 2005 to 2021 exhibit significant variations in certain regions, despite identical

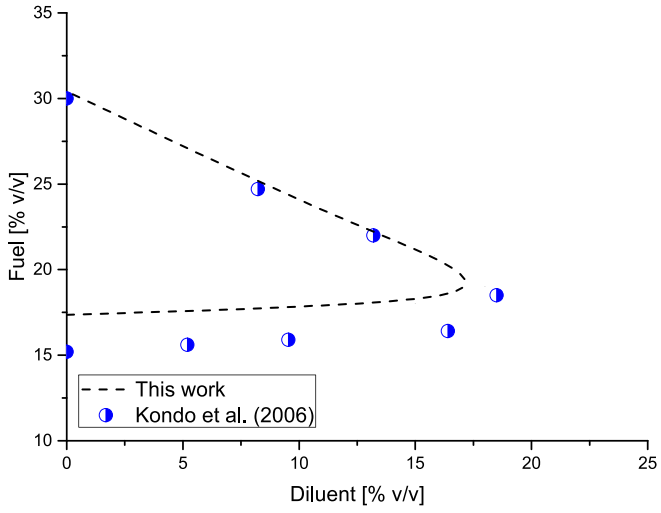

Fig. 3. Comparison of experimental and numerical flammability region for ammonia-oxygen–nitrogen mixtures at an initial temperature of 300 K and initial pressure of 1 bar, as a function of the additional nitrogen.

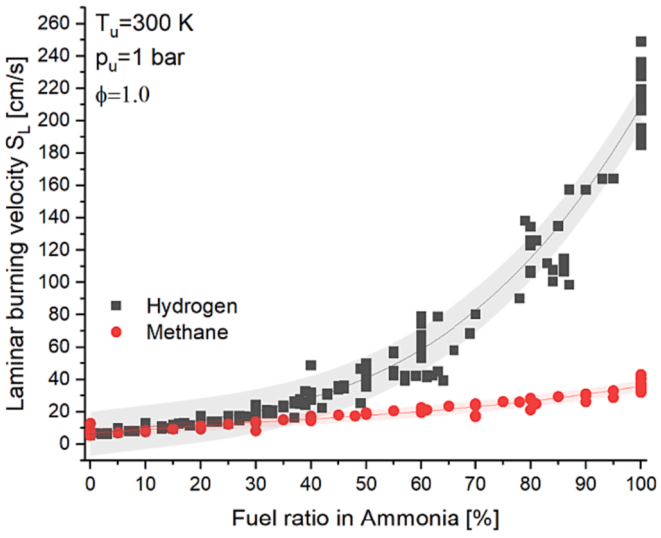

Fig. 4. The effect of the presence of ammonia on the initial fuel composition on the laminar burning velocity at stoichiometric composition, 300 K, and 1 bar.

conditions, with discrepancies of up to 30 %. The difference between the observed trends can be attributed to the similarity in the overall reactivity of methane and ammonia, which are significantly lower than hydrogen under the investigated conditions. Nevertheless, the significance of the impact of an addition of hydrogen is limited on ammonia-containing mixtures, in line with the trends observed in the literature for the case of methane-hydrogen binary mixtures [57], especially at stoichiometric composition. Besides, similar values can be observed for Mix 4 and Mix 6 once extremely rich compositions are considered, as reported in Figures S23 and S25. Therefore, it is possible to conclude that the addition of hydrogen or ammonia to methane leads to negligible effects on the laminar burning velocity. Hence, a limited impact of chemical kinetic can be postulated. Conversely, the reactivity at the ultra-rich composition of the investigated binary mixture of ammonia e hydrogen (i.e., Mix 5) follows a belt shape closer to the one observed for pure hydrogen. These observations are confirmed also by the comparison of flammability limits of the analysed species, as shown in panels d, e, and f of Figure S39. Under these premises, the discrepancies between the reported trends can be attributed to the difference in thermal properties, affecting the inertia of the initial mixtures.

3.3. Oxidation of ternary mixtures

For the sake of clarity, the effects of the equivalence ratio and oxygen-to-nitrogen ratio on the laminar burning velocity were reported for Mix 8 (Fig. 5), as obtained for 300 K and 1 bar. The selection of this composition as a base case condition can be intended for the evaluation of short-term solutions because of its plausible utilization within existing technologies for gas transportation. Besides, the previously presented results indicated a similar behaviour for methane-rich fuels, regardless of the added species. Therefore, Mix 8 can be intended as representative of any ternary mixtures showing a methane-dominated chemistry. Nevertheless, the full set of data related to the corresponding estimations for all the ternary mixtures investigated in this work is reported in the supplementary material (Figures S26-S38).

Considering the focus of this work on the safety aspects, more emphasis will be given to the discussion on lean and rich compositions providing laminar burning velocities in the proximity of the limiting values. Nevertheless, it is worth mentioning that the equivalence ratio leading to a peak in the estimated laminar burning velocity is weakly affected by the initial composition of the oxidant agent, being at a slightly rich composition for all the investigated conditions. Besides, the

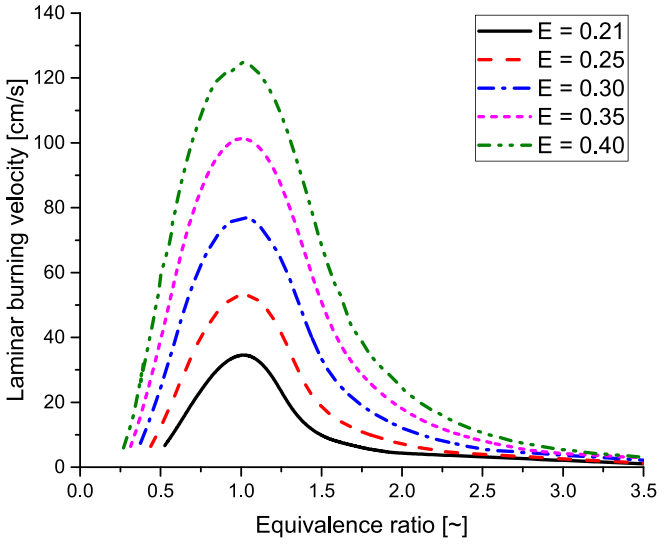

Fig. 5. The effects of initial composition in terms of equivalence ratio and oxygen content on the laminar burning velocity of Mix 8 (namely 5 %v of H_2, 5 %v of NH_3 in CH_4) at 300 K and 1 bar.

effects of E on the maximum laminar burning velocity ($S_{L,\max}$) are well described by Equation (4).

$$S_{L,max} = 476.3 \bullet E - 65.5 \quad (4)$$

Similarly, the pressure dynamic, in terms of the maximum pressure rise rate and the maximum pressure, achieved by Mix 8 as a function of the initial temperature and E are provided in Fig. 6. For the sake of discussion, data corresponding to an initial temperature of 300 K and E of 0.21 are also reported for binary and ternary mixtures investigated in this work.

While an enhancement in the initial temperature results in a decrease in the maximum pressure due to an altered ratio between adiabatic flame temperature and the initial temperature, this modification in the initial conditions concurrently induces a more critical scenario in terms of structure integrity and explosive hazards, as evidenced by the observed trend in the maximum pressure rise rate. Regarding the effects of air enrichment on pressure dynamics, an increase in E induces larger maximum pressures and maximum pressure rise rates. In this sense, the increase in the estimated P_{max} can be attributed to the higher adiabatic flame, whereas the observed trend in $\left(\frac{dP}{dt}\right)_{max}$ can be associated with a reduction in the flame thickness due to the faster kinetic. Upon comparing these parameters across various initial compositions, it becomes evident that Mix 9 emerges as the most critical composition, primarily due to its substantial hydrogen fraction. This assertion is substantiated by sorting the investigated mixtures by $\left(\frac{dP}{dt}\right)_{max}$ revealing the highest values when the initial hydrogen content exceeds 35 % volume within the fuel mixture. However, it is important to note that when considering P_{max}, Mix 11 exhibits larger values despite its hydrogen content being limited to 10 % volume. The combination of these tendencies can be attributed to the chemistry at a radical level of the investigated species. Indeed, the presence of hydrogen in a methane-rich mixture provides a large source of abstracting agents, which promotes the activation of methane, with obvious implications on the overall reactivity and flame thickness. Similarly, a larger content of hydrogen is needed when dealing with ammonia, as reported in the literature for the binary mixtures of hydrogen and ammonia, where a regime dominated by the H and OH radicals was distinguished by one ruled by NH_2 and OH [58]. Once lean compositions are analysed, a linear trend concerning the equivalence ratio can be observed, regardless of the level of oxygen considered in the oxidant mixture. Conversely, the increase in the oxygen-to-nitrogen ratio leads to modified curve shapes for the rich case. In particular, the reported data clearly indicate the significant impact of oxygen content on the overall reactivity of the analysed mixtures. This observation can be associated with a thermal effect, namely because of the reduced thermal inertia due to the lower content of nitrogen, as well as to a chemical effect, due to the increase in the concentration of oxygen. Considering the similarity in the calculated adiabatic flame temperature, which will be also discussed later in this section, the latter alternative seems to play a larger role in the determination of the laminar burning velocity. In this light, the larger impact of this parameter on the rich flames than on lean flames corroborates this assumption since oxygen represents the limiting reactant in rich conditions, only. Besides, the achievement of the asymptotic value for the laminar burning velocity is less evident and shifted toward a larger equivalence ratio. In principle, this trend suggests that LFL can be less affected by the use of different oxidants than UFL. However, the modified composition of the reactants due to the increase in E can reasonably affect the limiting laminar burning velocity. For these reasons, additional insights will be provided on this aspect once the flammability limits are reported. In addition, the observed trends discussed in this section for Mix 8 are qualitatively representative of any ternary mixtures having at least 80 %v of a single fuel (i.e., Mix 9, Mix 10, Mix 11, Mix 12, and Mix 13). Conversely, the remaining mixtures (i.e., Mix 7, Mix 14, Mix 15, Mix 16, Mix 17, Mix 18, and Mix 19) do not present any region showing a behaviour dominated by a single component. Besides, a

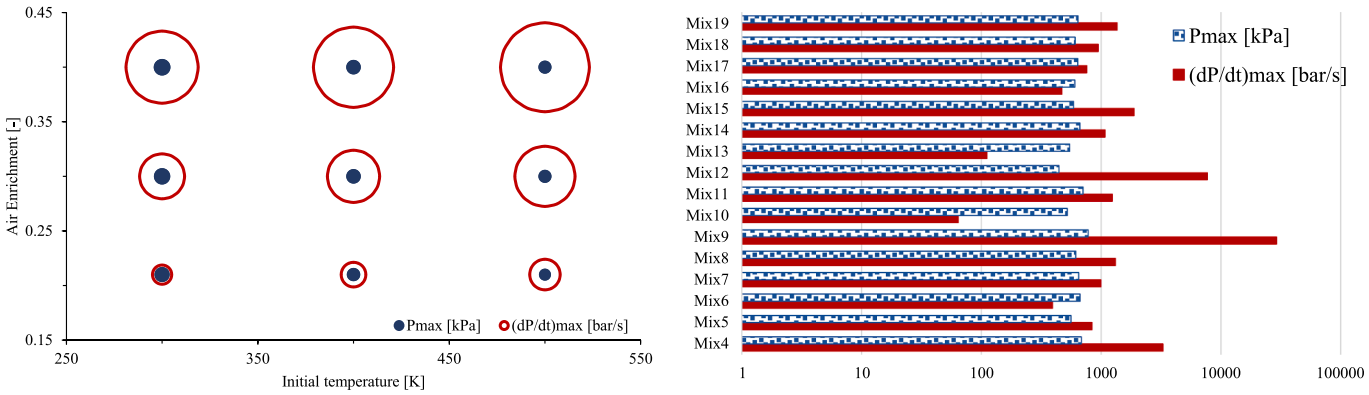

Fig. 6. Maximum pressure rise rate and maximum pressure obtained for: Mix 8 as a function of initial temperature and oxidant composition, at an equivalence ratio equal to 1 (left); fuel mixtures investigated in this work at an initial temperature of 300 K, in air, and stoichiometric composition (right).

synergistic effect of the simultaneous presence of ammonia and methane in the initial mixture can be observed. Indeed, the reactivity of hydrogen is hindered by the presence of less reactive species. Similar data were obtained at different initial temperatures and for the fuel mixtures defined in the methodological section. Regardless of the analysed composition, the collected data indicate that the increase in initial temperature does not lead to a significant alteration of the belt-shaped curve of the laminar burning velocity as a function of the equivalence ratio. Conversely, the initial fuel composition plays a more relevant role in the determination of the composition showing the maximum laminar burning velocity and the achievement of constant values in rich conditions. Increases in the initial temperature result in larger burning velocity. However, the quantification of this variation is affected by the initial composition, as demonstrated by the well-established empirical correlation accounting for the impact of the initial temperature (Equation (5).

$$S_L(T) = S_L(T_0) \bullet \left(\frac{T}{T_0}\right)^{\alpha} \tag{5}$$

where α is an empirical value determined by the composition of the initial mixture. Typically, the effects of initial composition and initial temperature on the burning velocity are distinguished into different correlations. However, considering that $S_L(T_0)$ depends also on the initial composition, a unified equation was proposed in this work. The effect of initial composition was evaluated based on the available correlations. Indeed, previous investigations have identified the Gulder [59] equation, as modified by Coppens et al. [60], as the most convenient option for the evaluation of the laminar burning velocity of methane-hydrogen-air mixtures at low initial temperatures [57]. In addition, robust and detailed analyses dealing with the quantification of fitting parameters are available in the literature for fuel mixtures considering methane as a primary species. For these reasons, this correlation was considered in this work to reproduce the analysed mixtures. Furthermore, an additional term was included to account for the initial composition of the oxidant following the structure considered for the evaluation of the initial temperature, resulting in the merged correlation reported below (Equation (6):

$$S_{L,mix}(T) = \left[W \cdot \varphi^{\eta} exp^{-\xi\left(\varphi-\sigma-\sum_i x_i\Omega_i\right)^2} \cdot \prod_i [(1+\gamma_i \cdot x_i^{\tau_i})]\right] \bullet \left(\frac{T}{T_0}\right)^{\alpha} \cdot \left(\frac{E}{E_0}\right)^{\delta} \tag{6}$$

where W, η, ξ and σ are empirical coefficients related to the main fuel, assumed as methane in this work and retrieved from the current literature [57]; Ω_i, γ_i and τ_i refer to the additional fuel (i.e., hydrogen and ammonia); δ and α are functions related to temperature and enrichment index defined as Equation (7) and Equation (8), respectively.

$$\delta = E_1 + E_2 \bullet \varphi + E_3 \bullet \varphi^2 \tag{7}$$

$$\alpha = T_1 + T_2 \bullet \varphi + T_3 \bullet \varphi^2 \tag{8}$$

where E_1, E_2, E_3, T_1, T_2, and T_3 are constants deriving from the fitting procedure. The collected data were adopted to determine the defined coefficients within the flammable regions that will be discussed in detail later in this work. The coefficients reported in Table 1 were found to minimize the differences between the numerical estimations and the results deriving from the empirical correlation, leading to an overall coefficient of determination (R^2) larger than 0.95.

The estimated values for the laminar burning velocity and adiabatic flame temperature were, then, considered for the assessment of the flammability limits. It is worth mentioning that the implementation of different methods for the estimation of flammability limits leads to an almost negligible difference in most of the cases, namely within ± 5 % in terms of composition. In addition, the adiabatic flame temperature calculated at the compositions resulted in $S_L = S_{L,lim}$ lied within the range of initial temperature + 930 K, confirming the validity of the posed threshold value under the investigated conditions. In Fig. 7, the evolution of the Lower Flammable Limit (LFL) and Upper Flammable Limit (UFL) as a function of the mixture composition is observed. The region depicted by each bar represents the reactive range, where combustion can occur. Below this range, extinguishment results from a deficiency of fuel, whereas above it, extinguishment is due to an oxygen deficiency.

Numerical results obtained in this work produce a slightly more conservative figure than the experimental data available for the pure mixtures, e.g., Coward and Jones (1952) [61] and Zlochower et al. [10] for methane, and Ciccarelli et al. [62] for hydrogen and ammonia. However, it is worth noting that none of the compositions lead to variations in LFL larger than 10 %, whereas variations larger than 40 % can be observed also for ternary mixtures once UFL is considered.

Table 1
Parameters calculated in this work for the evaluation of the laminar burning velocity of mixtures containing ammonia in methane.

Parameter	
Ω_{NH_3}	−0.19
γ_{NH_3}	0.15
τ_{NH_3}	−0.01
E_1	3.25
E_2	−4.25
E_3	2.81
T_1	4.18
T_2	−4.33
T_3	1.90

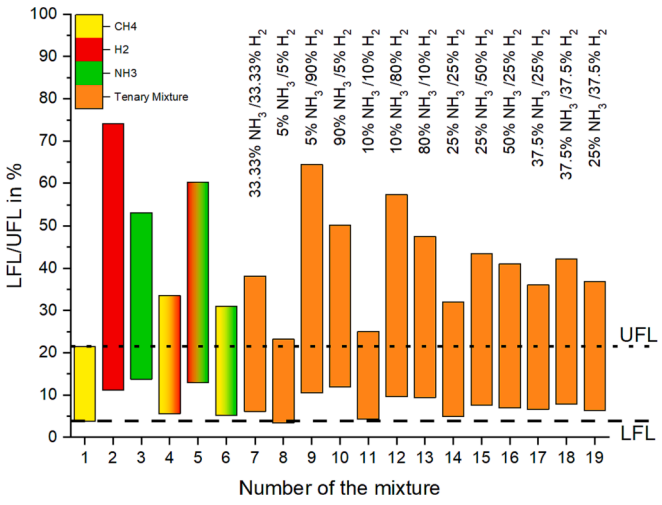

Fig. 7. Comparison of the flammability limits obtained for the investigated mixtures.

Furthermore, the effects of composition on the LFL were found mainly due to the proportion of NH_3. Conversely, UFL clearly depends on the H_2 content in the mixtures, because of the augmented availability of radicals involved in ignition phenomena, thus increasing the resulting UFL. It is evident that mixtures dominated by ammonia exhibit a tendency toward higher LFL values in several areas. However, the presence of NH_3 and H_2 significantly enhances the upper flammability limit. In general, the addition of NH_3 and H_2 leads to a notable broadening of the flammability range, which can be attributed to the large availability of H radicals acting as initiator agents.

For the sake of conciseness, once the effect of the initial composition of the oxidant is of concern, only the flammable region obtained for the ternary mixture referred to as Mix 8 as a function of the initial temperature is reported in Fig. 8. However, homologous data corresponding to the other mixtures investigated in this work can be found in the supplementary material. Conversely, the effects of the initial composition on the minimum oxygen concentration (MOC) potentially leading

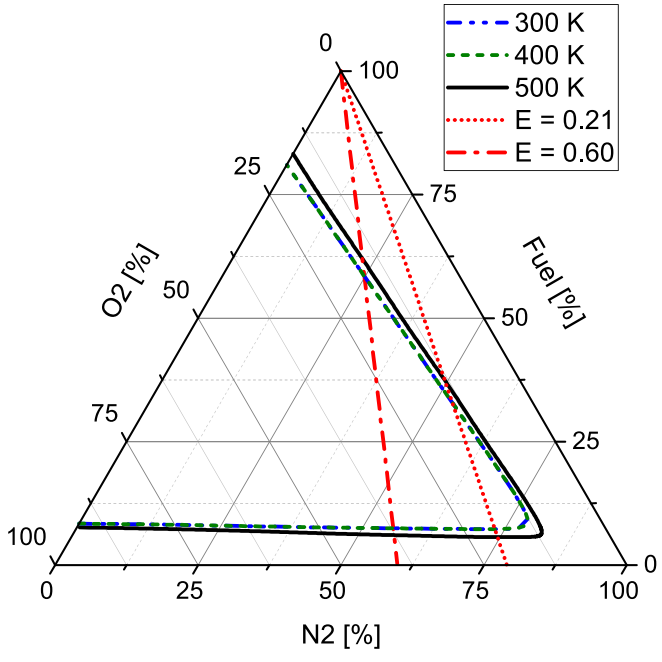

Fig. 8. Flammability region of Mix 8 as a function of the oxidant composition and initial temperature.

to a stable flame are reported in Table 2, as obtained at 300 K. Experimental data available in the current literature [10,63], as well as estimations deriving from the well-known stoichiometric correlation suggested by Li et al. [64], were added for the sake of comparison.

It is noteworthy that the influence of the initial temperature on the LFL is nearly negligible when the nitrogen content is below 50 %v (corresponding to E ~ 0.65). In contrast, the UFL experiences a considerable increase with variations in the initial temperature, even when pure oxygen is considered as the oxidant. Considering that LFL is typically determined by thermal aspects and UFL by kinetic aspects, the differences in observed trends demonstrate that nitrogen assumes a more substantial role as a heat sink compared to the chemical diluent at the investigated conditions. These trends were confirmed by data reported in supplementary material referring to the effect of initial conditions on the flammability region (Figure S39). Regardless of the initial temperature considered, a linear trend with respect to the oxygen-to-nitrogen ratio can be observed either for the lower or the upper flammability limits. Besides, under the investigated conditions, the effect of initial temperature on the flammable region of ternary fuel mixtures is limited, showing a slight increase with larger temperatures. Once the effects of the initial composition on the obtained MOC are analysed, the implementation of different approaches leads to significantly different results. In particular, it is worth mentioning that the empirical correlation considered in this work tends to significantly underestimate the MOC, meaning that this approach represents a conservative method on the safe side. However, larger accuracy can be observed by the use of a detailed kinetic mechanism, especially once the hydrogen is included within the initial mixture.

In the future, multi-component systems are poised to play a significantly expanded role in various applications. Currently, a robust experimental database is lacking, especially in cases involving oxygen enrichment or substantial additions of NH_3 or H_2. Consequently, there is a pressing need to numerically compute this data. In this context, as in other fields, the application of predictive methods using machine learning techniques may assume a more prominent role, as successfully demonstrated by similar applications in the field [65]. Nevertheless, the combination of newly generated correlations with detailed kinetic studies guarantees a robust characterization of safety aspects and combustion control. Indeed, a nuanced understanding of the chemistry inherent to the gaseous system is integral to the success of this numerical study. By incorporating detailed chemical kinetics models, the simulations provide a holistic view of combustion processes, allowing for the identification of key chemical factors influencing flammability, overall

Table 2
Minimum oxygen concentration (MOC) at 300 K as a function of the initial composition and numerical methods.

Mixture	Minimum oxygen concentration (MOC) [%v]		
	Kinetic mechanism	Empirical correlation	Experimental data
Mix 1	12.7	10.0	11.1
Mix 2	4.6	2.5	4.6
Mix 3	12.9	11.7	12.2
Mix 4	9.5	8.6	9.1
Mix 5	10.4	9.3	
Mix 6	13.3	10.5	
Mix 7	11.8	9.2	
Mix 8	13.2	9.9	
Mix 9	7.6	6.2	
Mix 10	12.7	11.7	
Mix 11	13.4	9.9	
Mix 12	9.0	6.8	
Mix 13	12.3	11.1	
Mix 14	12.5	9.5	
Mix 15	11.2	8.4	
Mix 16	11.7	9.7	
Mix 17	12.0	9.5	
Mix 18	11.7	8.8	
Mix 19	11.5	9.1	

reactivity and pressure dynamics in the case of ignition.

4. Conclusions

This study offers a novel exploration into the chemical behaviour of gaseous mixtures devoid of carbon compounds, specifically hydrogen and ammonia, in an oxidizing environment. Various combinations of fuels, oxidants, and operational parameters were thoroughly investigated. By employing a meticulously developed and validated kinetic model, the overall reactivity and flammability boundaries were ascertained. The availability of a robust toolkit for quantifying the reactivity of lightweight species across a broad spectrum of conditions opens up fresh avenues for innovative and robust designs in chemical production processes. Based on the collected results, simplified correlations were developed. The ruling chemistry and the possible key parameters to be considered for an accurate representation of accidental releases involving synthetic gaseous fuels were identified in this study. The adopted methodology stands as a comprehensive and interdisciplinary approach for rigorously validating precise models, enabling the comprehensive characterization of reactivity and safety aspects throughout the entire life cycle. Consequently, these findings hold significant promise for enhancing processes and techniques across various industrial domains.

CRediT authorship contribution statement

Gianmaria Pio: . **Sven Eckart:** Writing – review & editing, Visualization, Conceptualization. **Andreas Richter:** Writing – review & editing, Supervision. **Hartmut Krause:** Writing – review & editing, Resources, Project administration. **Ernesto Salzano:** Writing – review & editing, Supervision, Project administration.

Declaration of Competing Interest

The authors declare that they have no known competing financial interests or personal relationships that could have appeared to influence the work reported in this paper.

Data availability

Data will be made available on request.

Appendix A. Supplementary material

Supplementary data to this article can be found online at https://doi.org/10.1016/j.fuel.2023.130747.

References

[1] United Nations. Paris agreement. Paris; 2015.
[2] Lee HC, Mohamad AA, Jiang LY. A detailed chemical kinetics for the combustion of H2/CO/CH4/CO2fuel mixtures. Fuel 2017;193:294–307. https://doi.org/10.1016/j.fuel.2016.12.062.
[3] Mashruk S, Vigueras-Zuniga MO, Tejeda-del-Cueto ME, Xiao H, Yu C, Maas U, et al. Combustion features of CH4/NH3/H2 ternary blends. Int J Hydrogen Energy 2022;47:30315–27. https://doi.org/10.1016/j.ijhydene.2022.03.254.
[4] Hayakawa A, Goto T, Mimoto R, Arakawa Y, Kudo T, Kobayashi H. Laminar burning velocity and Markstein length of ammonia/air premixed flames at various pressures. Fuel 2015;159:98–106. https://doi.org/10.1016/j.fuel.2015.06.070.
[5] Salzano E, Pio G, Ricca A, Palma V. The effect of a hydrogen addition to the premixed flame structure of light alkanes. Fuel 2018;234:1064–70. https://doi.org/10.1016/j.fuel.2018.07.110.
[6] Eckart S, Rong FZ, Hasse C, Krause H, Scholtissek A. Combined experimental and numerical study on the extinction limits of non-premixed H2/CH4 counterflow flames with varying oxidizer composition. Int J Hydrogen Energy 2023;48:14068–78. https://doi.org/10.1016/j.ijhydene.2022.12.061.
[7] Han JW, Lee CE, Kum SM, Hwang YS. Study on the improvement of chemical reaction mechanism of methane based on the laminar burning velocities in OEC. Energy Fuel 2007;21:3202–7. https://doi.org/10.1021/ef070175v.
[8] Belaissaoui B, Le Moullec Y, Hagi H, Favre E. Energy efficiency of oxygen enriched air production technologies: cryogeny vs membranes. Energy Procedia 2014;63:497–503. https://doi.org/10.1016/j.egypro.2014.11.054.
[9] Nur HFMZ, Rafiziana KM, Azeman M. Numerical investigation on laminar burning velocity of hydrogen-methane / air mixtures : a review 2015:40–9.
[10] Zlochower IA, Green GM. The limiting oxygen concentration and flammability limits of gases and gas mixtures. J Loss Prev Process Ind 2009;22:499–505. https://doi.org/10.1016/j.jlp.2009.03.006.
[11] Cheng Y, Tang C, Huang Z. Kinetic analysis of H2addition effect on the laminar flame parameters of the C1–C4 n-alkane-air mixtures: from one step overall assumption to detailed reaction mechanism. Int J Hydrogen Energy 2015;40:703–18. https://doi.org/10.1016/j.ijhydene.2014.11.010.
[12] Schenk M, Leon L, Moshammer K, Oßwald P, Zeuch T, Seidel L, et al. Detailed mass spectrometric and modeling study of isomeric butene flames. Combust Flame 2013;160:487–503. https://doi.org/10.1016/j.combustflame.2012.10.023.
[13] Pio G, Dong X, Salzano E, Green WH. Automatically generated model for light alkene combustion. Combust Flame 2022;241:112080. https://doi.org/10.1016/j.combustflame.2022.112080.
[14] Gilbert A. Introduction to computational quantum chemistry: theory. Phys Rev 2007.
[15] Benson SW. Thermochemical Kinetics: Methods for the Estimation of Thermochemical Data and Rate Parameters. Thermochem. Kinet. 2nd ed., Hoboken, USA: John Wiley & Sons, Inc.; 1976. https://doi.org/10.1002/BBPC.19690730226.
[16] Ramakrishnan R, Dral PO, Rupp M, Von Lilienfeld OA. Big data meets quantum chemistry approximations: the Δ-machine learning approach. J Chem Theory Comput 2015;11:2087–96. https://doi.org/10.1021/acs.jctc.5b00099.
[17] Wako FM, Pio G, Salzano E. Modelling of acetaldehyde and acetic acid combustion. Combust Theory Model 2023;27:536–57. https://doi.org/10.1080/13647830.2023.2178973.
[18] Gao CW, Allen JW, Green WH, West RH. Reaction mechanism generator: automatic construction of chemical kinetic mechanisms. Comput Phys Commun 2016;203:212–25. https://doi.org/10.1016/j.cpc.2016.02.013.
[19] Eckart S, Pio G, Zirwes T, Zhang F, Salzano E, Krause H, et al. Impact of carbon dioxide and nitrogen addition on the global structure of hydrogen flames. Fuel 2023;335:126929. https://doi.org/10.1016/j.fuel.2022.126929.
[20] Pio G, Ricca A, Palma V, Salzano E. Low temperature combustion of methane/alkenes mixtures. Fuel 2019;254:115567.
[21] Xu C, Konnov AA. Validation and analysis of detailed kinetic models for ethylene combustion. Energy 2012;43:19–29. https://doi.org/10.1016/j.energy.2011.11.006.
[22] Yu C, Eckart S, Essmann S, Markus D, Valera-Medina A, Schießl R, et al. Investigation of spark ignition processes of laminar strained premixed stoichiometric NH3-H2-air flames. J Loss Prev Process Ind 2023;83:105043. https://doi.org/10.1016/j.jlp.2023.105043.
[23] Selle L, Poinsot T, Ferret B. Experimental and numerical study of the accuracy of flame-speed measurements for methane/air combustion in a slot burner. Combust Flame 2011;158:146–54. https://doi.org/10.1016/j.combustflame.2010.08.003.
[24] Hu E, Li X, Meng X, Chen Y, Cheng Y, Xie Y, et al. Laminar flame speeds and ignition delay times of methane–air mixtures at elevated temperatures and pressures. Fuel 2015;158:1–10. https://doi.org/10.1016/j.fuel.2015.05.010.
[25] Mitu M, Razus D, Giurcan V, Oancea D. Normal burning velocity and propagation speed of ethane-air: pressure and temperature dependence. Fuel 2015. https://doi.org/10.1016/j.fuel.2015.01.026.
[26] Kim GT, Il KN. Laminar burning velocity predictions by meso-scale flames in an annular diverging tube. Fuel 2011;90:2217–23. https://doi.org/10.1016/j.fuel.2011.02.039.
[27] Liu Z, Il KN. An assembled annular stepwise diverging tube for the measurement of laminar burning velocity and quenching distance. Combust Flame 2014;161:1499–506. https://doi.org/10.1016/j.combustflame.2013.11.020.
[28] Eckart S, Cai L, Fritsche C, vom Lehn F, Pitsch H, Krause H. Laminar burning velocities, CO, and NOx emissions of premixed polyoxymethylene dimethyl ether flames. Fuel 2021;293:120321. https://doi.org/10.1016/j.fuel.2021.120321.
[29] Eckart S, Zsély IG, Krause H, Turányi T. Effect of the variation of oxygen concentration on the laminar burning velocities of hydrogen-enriched methane flames. Int J Hydrogen Energy 2023. https://doi.org/10.1016/j.ijhydene.2023.08.217.
[30] Konnov AA, Mohammad A, Kishore VR, Il KN, Prathap C, Kumar S. A comprehensive review of measurements and data analysis of laminar burning velocities for various fuel+air mixtures. Prog Energy Combust Sci 2018;68:197–267. https://doi.org/10.1016/j.pecs.2018.05.003.
[31] Eckart S, Penke C, Voss S, Krause H. Laminar burning velocities of low calorific and hydrogen containing fuel blends. Energy Procedia 2017;120:149–56. https://doi.org/10.1016/j.egypro.2017.07.148.
[32] Eckart S, Benaissa S, Alsulami RA, Juhany KA, Krause H, Mohammad A. Laminar burning velocity, emissions, and flame structure of dimethyl ether-hydrogen air mixtures. Int J Hydrogen Energy 2023;48:35771–85. https://doi.org/10.1016/j.ijhydene.2023.05.261.
[33] Egolfopoulos FN, Hansen N, Ju Y, Kohse-Hoinghaus K, Law CK, Qi F. Advances and challenges in laminar flame experiments and implications for combustion chemistry. Prog Energy Combust Sci 2014;43:36–67. https://doi.org/10.1016/j.pecs.2014.04.004.
[34] Perpignan AAV, Gangoli Rao A, Roekaerts DJEM. Flameless combustion and its potential towards gas turbines. Prog Energy Combust Sci 2018;69:28–62. https://doi.org/10.1016/j.pecs.2018.06.002.

[35] Pio G, Salzano E. The effect of ultra-low temperature on the flammability limits of a methane/air/diluent mixtures. J Hazard Mater 2019;362:224–9. https://doi.org/10.1016/j.jhazmat.2018.09.018.
[36] Hertzberg M. The theory of flammability limits, flow gradient effect and flame stretch. rep investig 8865 -. United States Dep Inter 1984:1–41.
[37] Vidal M, Wong W, Rogers WJ, Mannan MS. Evaluation of lower flammability limits of fuel-air-diluent mixtures using calculated adiabatic flame temperatures. J Hazard Mater 2006;130:21–7. https://doi.org/10.1016/j.jhazmat.2005.07.080.
[38] Shu G, Long B, Tian H, Wei H, Liang X. Flame temperature theory-based model for evaluation of the flammable zones of hydrocarbon-air-CO2 mixtures. J Hazard Mater 2015;294:137–44. https://doi.org/10.1016/j.jhazmat.2015.03.064.
[39] Ye M, Sharp P, Brandon N, Kucernak A. System-level comparison of ammonia, compressed and liquid hydrogen as fuels for polymer electrolyte fuel cell powered shipping. Int J Hydrogen Energy 2022;47:8565–84. https://doi.org/10.1016/j.ijhydene.2021.12.164.
[40] van den Bosch C, Weterings R. Yellow Book - Methods for the calculation of physical effects due to releases of hazardous materials (liquids and gases). CPR 14E, 3rd Edn, TNO 1997.
[41] Molkov V, Saffers J. Hydrogen jet flames. Int J Hydrogen Energy 2012;38:8141–58. https://doi.org/10.1016/j.ijhydene.2012.08.106.
[42] Pio G, Ruocco C, Palma V, Salzano E. Detailed kinetic mechanism for the hydrogen production via the oxidative reforming of ethanol. Chem Eng Sci 2021;237:116591. https://doi.org/10.1016/j.ces.2021.116591.
[43] Green Book - Guidelines for Quantitative risk assessment. Methods for the determination of possible damage n.d.
[44] Wako FM, Pio G, Salzano E. Modeling formic acid combustion. Energy Fuel 2022;36:14382–92. https://doi.org/10.1021/acs.energyfuels.2c03249.
[45] Pio G, Palma V, Salzano E. Comparison and validation of detailed kinetic models for the oxidation of light alkenes. Ind Eng Chem Res 2018;57:7130–5.
[46] Goodwin DG. An Open Source, Extensible Software Suite FOR CVD Process Simulation. 2003.
[47] Masri AR. Challenges for turbulent combustion. Proc Combust Inst 2021;38:121–55. https://doi.org/10.1016/j.proci.2020.07.144.
[48] Iso 6976. bs en iso 6976,. 2016 BSI Standards Publication Natural gas — Calculation of calorific values, density. relative density and Wobbe indices from composition. 2016.
[49] Han J, Bai L, Yang B, Bai Y, Luo S, Zeng S, et al. Highly selective oxygen/nitrogen separation membrane engineered using a porphyrin-based oxygen carrier. Membranes (Basel) 2019;9:115. https://doi.org/10.3390/membranes9090115.
[50] Li R, Liu Z, Han Y, Tan M, Xu Y, Tian J, et al. Extended adiabatic flame temperature method for lower flammability limits prediction of fuel-air-diluent mixture by nonstoichiometric equation and nitrogen equivalent coefficients. Energy Fuel 2017;31:351–61. https://doi.org/10.1021/acs.energyfuels.6b02459.
[51] Razus D, Molnarne M, Movileanu C, Irimia A. Estimation of LOC (limiting oxygen concentration) of fuel-air-inert mixtures at elevated temperatures by means of adiabatic flame temperatures. Chem Eng Process 2006;45:193–7. https://doi.org/10.1016/j.cep.2005.06.010.
[52] Pfahl UJ, Ross MC, Shepherd JE, Pasamehmetoglu KO, Unal C. Flammability limits, ignition energy, and flame speeds in H2-CH4-NH3- N2O–O2-N2 mixtures. Combust Flame 2000. https://doi.org/10.1016/S0010-2180(00)00152-8.
[53] Takizawa K, Takahashi A, Tokuhashi K, Kondo S, Sekiya A. Burning velocity measurements of nitrogen-containing compounds. J Hazard Mater 2008;155:144–52. https://doi.org/10.1016/j.jhazmat.2007.11.089.
[54] Szanthoffer AG, Zsély IG, Kawka L, Papp M, Turányi T. Testing of NH3/H2 and NH3/syngas combustion mechanisms using a large amount of experimental data. Appl Energy Combust Sci 2023;14:100127. https://doi.org/10.1016/j.jaecs.2023.100127.
[55] Kondo S, Takizawa K, Takahashi A, Tokuhashi K. Extended Le Chatelier's formula and nitrogen dilution effect on the flammability limits. J Hazard Mater 2006;138:1–8. https://doi.org/10.1016/j.jhazmat.2006.05.035.
[56] Chen CC. A study on estimating flammability limits in oxygen. Ind Eng Chem Res 2011;50:10283–91. https://doi.org/10.1021/ie102373g.
[57] Pio G, Salzano E. Laminar burning velocity of methane, hydrogen, and their mixtures at extremely low-temperature conditions. Energy Fuel 2018;32:8830–6. https://doi.org/10.1021/acs.energyfuels.8b01796.
[58] Liang B, Yang M, Gao W, Jiang Y, Li Y. Study on premixed hydrogen-ammonia-air flame evolution in a horizontal rectangular duct. Fuel 2023;354. https://doi.org/10.1016/j.fuel.2023.129427.
[59] Gulder OL. Correlations of laminar combustion data for alternative S.I. engine fuels. SAE Tech Pap 1984.
[60] Coppens FHV, De Ruyck J, Konnov AA. Effects of hydrogen enrichment on adiabatic burning velocity and NO formation in methane + air flames. Exp Therm Fluid Sci 2007;31:437–44. https://doi.org/10.1016/j.expthermflusci.2006.04.012.
[61] Coward HF, Jones GW. Limits of flammability of gases and vapors. [Tables and graphs for organic and inorganic materials and mixtures; bibliography; indexes]. U.S. Department of Energy 1952. https://doi.org/10.2172/7355338.
[62] Ciccarelli G, Jackson D, Verreault J. Flammability limits of NH3-H2-N2-air mixtures at elevated initial temperatures. Combust Flame 2006;144:53–63. https://doi.org/10.1016/j.combustflame.2005.06.010.
[63] Molnarne M, Schroeder V. Flammability of gases in focus of European and US standards. J Loss Prev Process Ind 2017;48:297–304. https://doi.org/10.1016/j.jlp.2017.05.012.
[64] Li P, Liu Z, Li M, Zhao Y, Li X, Wan S, et al. Investigation on the limiting oxygen concentration of combustible gas at high pressures and temperatures during oil recovery process. Energy 2021;215:119157. https://doi.org/10.1016/j.energy.2020.119157.
[65] Prieler R, Moser M, Eckart S, Krause H, Hochenauer C. Machine learning techniques to predict the flame state, temperature and species concentrations in counter-flow diffusion flames operated with CH4/CO/H2-air mixtures. Fuel 2022;326:124915. https://doi.org/10.1016/j.fuel.2022.124915.